Engineering Geology 116 (2010) 95–108

Contents lists available at ScienceDirect

Engineering Geology

journal homepage: www.elsevier.com/locate/enggeo

Spatial distribution analysis of landslides triggered by 2008.5.12 Wenchuan Earthquake, China

Shengwen Qi [a,b,*], Qiang Xu [b], Hengxing Lan [c], Bing Zhang [d], Jianyou Liu [a,1]

[a] Key Lab. of Engineering Geomechanics, Institute of Geology and Geophysics, Chinese Academy of Sciences, Beijing, China, P.O. Box 9825, Chaoyang area, Beijing, 100029, China
[b] State Key Lab. of Geo-hazard Prevention and Geo-environment Protection, Chengdu University of Technology, Chengdu, 610059, China
[c] State Key Laboratory of Resources and Environmental System, Institute of Geographic Sciences and Natural Resources Research, Chinese Academy of Sciences, Beijing, 100101, China
[d] Centre for Earth Observation and Digital Earth, Chinese Academy of Sciences, Beijing, 100190, China

ARTICLE INFO

Article history:
Received 15 July 2009
Received in revised form 18 July 2010
Accepted 30 July 2010
Available online 11 August 2010

Keywords:
2008.5.12 Wenchuan Earthquake
Slope
Landslide
Spatial analysis

ABSTRACT

The 2008.5.12 Wenchuan Earthquake (seismic magnitude M_w 7.9 according to the USGS) triggered a great number of landslides. A spatial database of landslides is built by interpreting the remote sensing (RS) data which covers 11 counties severely damaged by the earthquake with area of about 31,686.12 km^2. The geological settings of the study area are detailed mapped including geologic structure and lithology. The digital elevation model (DEM) of the study area with resolution of 30 m × 30 m is presented to address the topographic characteristics. Correlations between the occurrence of landslides with geological settings i.e. active faults (the coseismic surface ruptures), geological unit, slope gradient, slope elevation as well as slope aspect are analyzed using spatial modeling in GIS with the aids of field investigations. It can be concluded that the distance to the causative faults and slope gradient are much more important than other factors. Landslides are clustered distributed along the causative faults of F2 and F3, and landslides incidence are dramatically decreasing with the increasing of the distance to the causative faults. The landslides incidence has an obvious increase near the active faults i.e. F1. Landslide concentration (LC, landslides/km^2) has an obvious exponent increase with slope gradient. However, LC has no obvious relationship with geological unit and slope elevation; the difference of LC value in each geological unit (each slope elevation category) maybe have been the result affected by slope gradient for each geological unit (each slope elevation category) and distance of each geological unit (each slope elevation category) to causative fault zone. Isoseismal map reflects the incidence of landslides in some degree, and LC increases dramatically with Intensity increasing, almost all landslides occurred in the region above VI degree.

Statistics result also indicates that in the near field of causative faults, landslides tend to have the initial sliding direction similar to the movement of the causative faults. And preliminary study shows that landslides incidence varies in different slopes with different structure, and consequent slopes and obsequent slopes have a higher landslides incidence than other layered slopes.

1. Introduction

A devastating earthquake measured as M_w8.3 according to Chinese Earthquake Administration—CEA (M_w7.9according to the USGS) occurred in Wenchuan County, Sichuan Province in Southwest China at 2:28 pm on 12 May 2008 (Wang et al., 2009). The earthquake killed more than 69,225 people and left 374,640 injured and about 17,393 missed by April 25th, 2009 according to official statistics, and caused a tremendous damage in properties.

The earthquake struck along the middle segment of the Longmenshan (LMS) thrust belt, at the eastern margin of the Tibetan Plateau. Seismological data indicate that the rupture initiated in the southern LMS and propagated unilaterally toward the northeast on a ~33° dipping fault for ~300 km (Fig. 1).

The earthquake shook area is located in the mountainous region of northwest of Sichuan Province. It is characterized by rugged topography, steep high mountains, deep valleys and complicated geologic structures. The investigation revealed that more than 15,000 landslides were triggered by the earthquake resulting in immediate deaths of about 20,000 (Yin et al., 2009). The most of Beichuan City, one unique Qiang autonomous city in China, was ruined by two landslides triggered by earthquake and caused deaths of about 3000.

* Corresponding author. Key Lab. of Engineering Geomechanics, Institute of Geology and Geophysics, Chinese Academy of Sciences, Beijing, China, P.O. Box 9825, Chaoyang area, Beijing, 100029, China. Tel.: +86 10 8299 8055; fax: +86 10 62040574.
E-mail addresses: qishengwen@mail.iggcas.ac.cn (S. Qi), xq@cdut.edu.cn (Q. Xu), lanhx@lreis.ac.cn (H. Lan), zb@ceode.ac.cn (B. Zhang), liujianyou@mail.iggcas.ac.cn (J. Liu).
[1] Tel.: +86 10 8299 8713; fax: +86 10 62040574.

0013-7952/$ – see front matter © 2010 Elsevier B.V. All rights reserved.
doi:10.1016/j.enggeo.2010.07.011

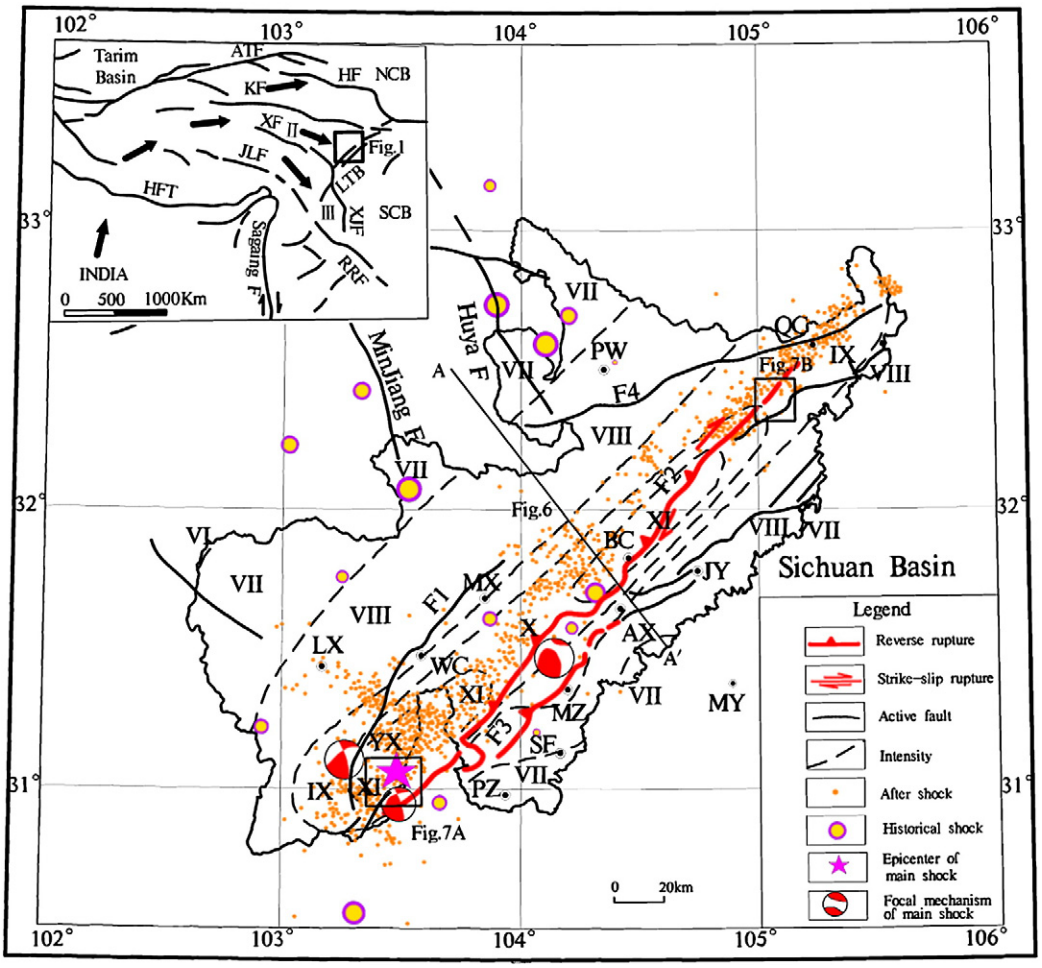

Fig. 1. Active tectonic map of the study area and the surface rupture zones induced by the earthquake (Revised after Xu et al., 2009). QC—Qingchuan City, PW—Pingwu City, JY—Jiangyou City, BC—Beichuan City, MX—Maoxian City, AX—Anxian City, MZ—Mianzhu, SF—Shifang City, PZ—Pengzhou City, WC—Wenchuan City, YX—Yingxiu town, Huya F—Huya Fault, Minjiang F—Minjiang Fault. F1—Maoxian–Wenchuan Fault, F2—Yingxiu–Beichuan Fault, F3—Guanxian–Anxian Fault, F4—Pingwu–Qingchuan Fault. Inset map shows major tectonic features in LMS vicinity: ATF—Altyn Tagh Fault, HF—Haiyuan Fault, JLF—Jiali Fault, LTB—Longmenshan thrust belt, NCB—North China block, RRF—Longmenshan thrust belt, KF—Kunlun Fault, SCB—South China block, XF—Xianshuihe Fault, XJF—Xiaojiang Fault, I—Qaidam–Qilian block, II—Bayan Har block, III—Sichuan–Yunnan block. Black arrow indicates block motion direction.

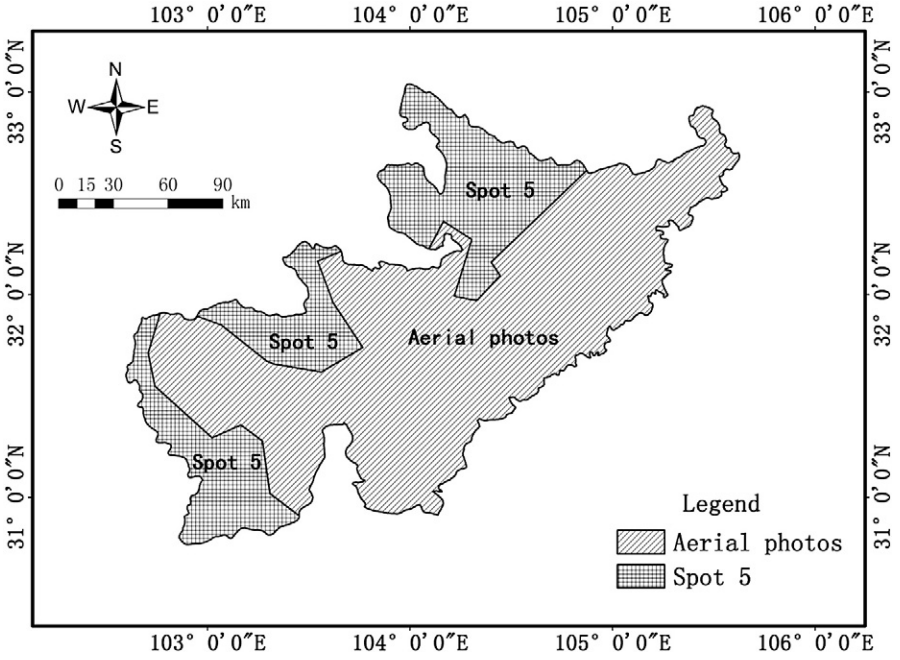

Fig. 2. The various RS data used in the study area.

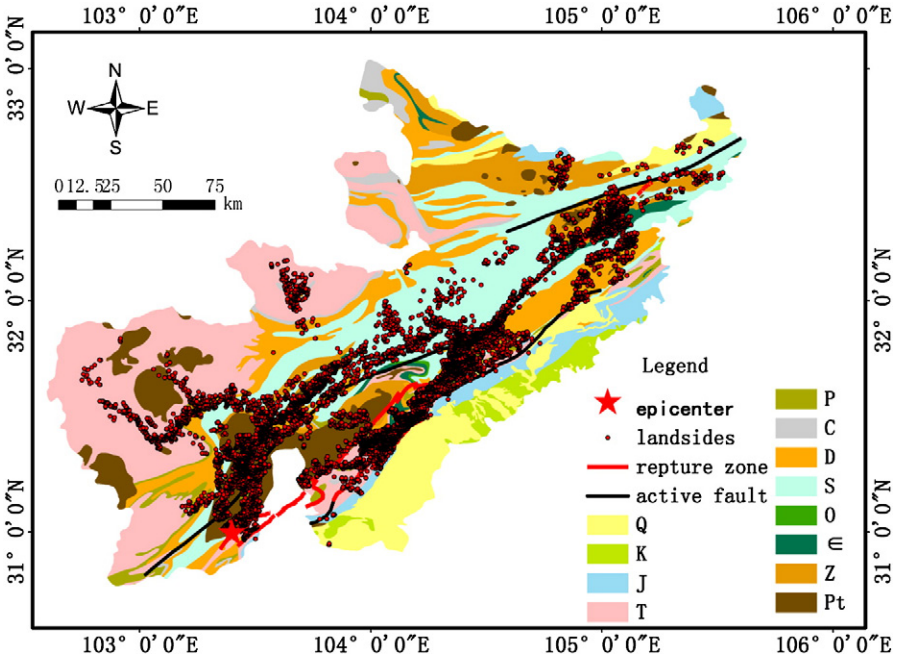

Fig. 3. Regional geological map of the severely damaged zone and landslides trigged by 2008 Wenchuan Earthquake (revised after CGS, 2001).

The first-hand and immediate information and data were extremely difficult to gain right after the Wenchuan Earthquake on May 12, 2008, due to the blocked transportation, the communication network cutting-off, numerous secondary disasters and severe weather conditions. Hence the remote sensing (RS) technology is playing a vital role in accessing the information in quake disaster areas. The RS data used in interpreting the landslides includes aerial photos of ADS40 with spatial resolution of 0.5 m and the color infrared acquired by the Center for Earth Observation and Digital Earth, Chinese Academy of Sciences, and satellite imageries obtained by French satellite SPOT-5 with a spatial resolution of 2.5 m. Using these abundant RS data obtained from May 16, 2008 to June 15, 2008, landslides triggered by the Wenchuan Earthquake in 11 most stricken counties with area of 31,686.12 km^2 were interpreted (see Fig. 2).

Based on the remote sensing interpretation, the detailed geological settings (the geological map with scale of 1:200,000) (China Geological Survey, CGS, 2001) and topography (with scale of 1:50,000) are mapped in GIS. Geostatistical methods (Keefer, 2000, 2002; Khazai and Sitar, 2003; Huang and Li, 2009; Sato and Harp, 2009) are used to analyze correlations between the distribution of landslides and geological settings i.e. distance from the causative fault (or the surface rupture zones), the movement of the surface rupture

Table 1
Simplified strata system of the severest damaged zone by 2008.5.12 Wenchaun earthquake (Summarized after Geological Bureau of Sichuan Province, 1991).

Sequence		Lithology
Cenozoic	Quaternary (Q)	Loose deposit
Mesozoic	Cretaceous (K)	Red strata bearing genebenthos facies, mainly consists of fine clastic rock, argillaceous rock, locally with coarse clastic rock and carbonate rock. Outcropped in Jiangyou, Anxian and Wenchuan.
	Jurassic (J)	Strata with river and lake facies clastic rock and mudstone facies. Mainly outcropped in Jiangyou, Anxian, Mianzhu, Shifang and Pengzhou. Additionally, sparsely outcropped in the Northeast of Qingchuan.
	Triassic (T)	Grey limestone; grey mudstone and sandy mudstone interlayering with silty sandstone and fine sandstone; thick feldspar quartzose sandstone interlayering with shale; grey middle thick metamorphic feldspar quartzose sandstone, interlayering with slate. Wildly outcropped in study area except Qingchuan.
Paleozoic	Permian (P)	Thick limestone intercalated slate, carbonate shale and clay stone. Sparsely outcropped in Mianzhu, Anxian, Jiangyou and Wenchuan
	Carboniferous (C)	Mainly epimetamorphic carbonate rock intercalated with clastic rock. Outcropped in Jiangyou, Mianzhu, Anxian, Beichuan, Maoxian and Pingwu.
	Devonian (D)	Metamorphic strata, carbonate rock and clastic rock non-uniform thickness interlayering each other, sparsely with middle basic volcanic rock. Mainly consists of grey argillaceous silty sandstone, silty sandy mudstone, and biocalcirudite. Outcropped in Jiangyou, Beichuan, Pingwu, Lixian and Wenchuan.
	Silurian (S)	Metamorphic strata mainly consists of marine facies clastic rock, siliceous rock, carbonate rock, flysch and volcanic clastic rock. Wildly outcropped in Qingchuan, Pingwu, Beichuan, Maoxian and Wenchuan; and sparsely outcropped in Anxian.
	Ordovician (O)	Thin-middle thick argillaceous limestone, sparsely outcropped in Beichuan, Anxian, Wenchuan and Maowen.
	Cambrian (∈)	Black siliceous phyllite; black silicalite intercalating siliceous slate; carbonaceous slate, silty slate and siliceous slate interbeded with dololite. Sparsely outcropped in Qingchuan, Pingwu, Beichuan, Maoxian and Wenchuan.
Proterozoic	Sinian (Z)	The lower series is formation of volcanic rock, pyroclastic rock and formation of tilly clastic rock, sparsely outcropped in Pengzhou, Maoxian and Wenchuan; the upper series is clastic rock formation and carbonate rock formation, mainly outcropped in Qingchuan and Pingwu, sparsely outcropped in Mianzhu and Anxian.
Archean (Pt)		Pengguan Massif, mainly a set of migmatized metamorphic rock and migmatite. Metamorphic rock consists of amphibolite, granulite and leucoleptite; migmatite consists of plagiogranite migmatite, adamellite migmatite etc. Outcropped in Anxian, Wenchuan, Mianzhu and Pengzhou and Lixian.

zones, strata sequence, slope gradient, slope elevation and slope aspect. Meanwhile, correlations between landslides and the isoseismal as well slope structure are preliminary studied.

2. Geological settings of the study area

The study area located in the eastern of Qinghai–Tibet Plateau, and the LMS fault zone crosses the study area with the strike direction about N40° E. It was well known that the continental collision between India and Eurasia in the Cenozoic has resulted in large crustal shortening across Asia (Molnar and Tapponnier, 1975; Molnar and Chen, 1978; Houseman and England, 1993; Kind et al., 2002; Li et al., 2008; Royden et al., 2008). GPS measurements confirm that crustal material is moving eastward in the east Tibetan Plateau (Zhang et al., 2004) and is obstructed by the rigid Sichuan basin of the Yangtze block (Copley and McKenzie, 2007). And then the LMS fault zone acted as the boundary between the east Tibetan Plateau and the Yangtze block. Meanwhile, the LMS fault zone is also known as a transitional boundary of crustal thickness and a high gravity gradient zone. In less than 100 km distance from west to east, the crustal thickness changes from 60–65 km to ~40 km (Xu et al., 2007; Yao et al., 2008), and the Bouguer gravity anomalies for Airy compensation changes from ~−300 mgal to ~−100 mgal (Jiang and Yu, 2005).

The LMS fault zone is composed of a series of compression or compresso-shear faults and folds. The most active faults include Maoxian–Wenchuan Fault (F1), Yingxiu–Beichuan Fault (F2),

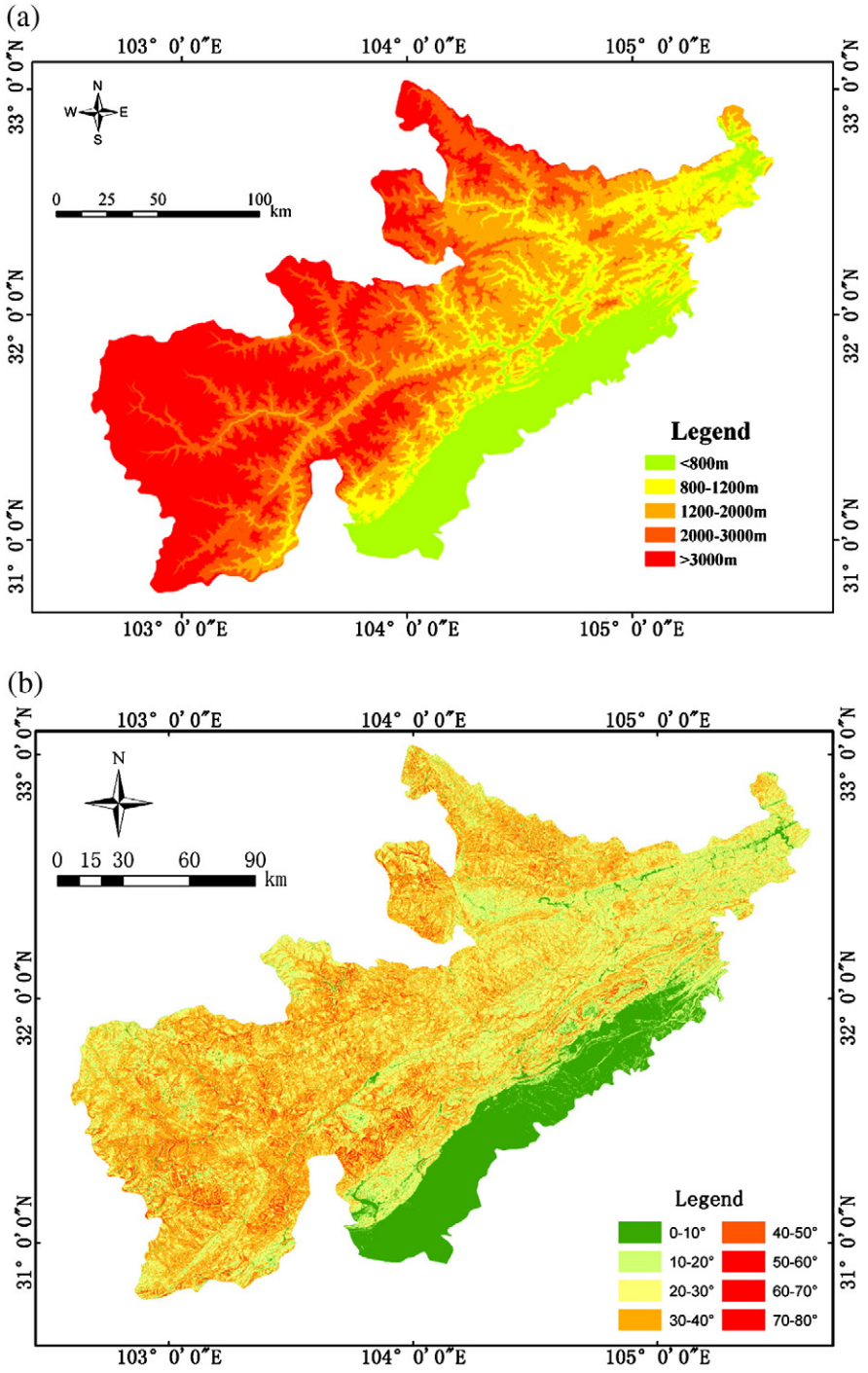

Fig. 4. (a) Digital elevation model (DEM) of the study area (After Qi et al., 2009); (b) Slope gradient distribution of the study area; (c) Slope aspect distribution of the study area.

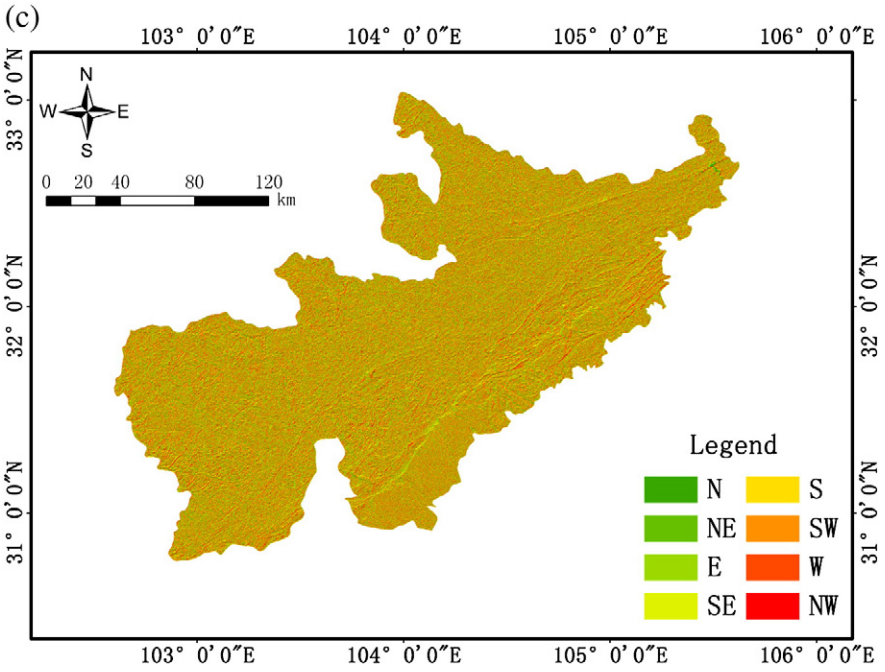

Fig. 4 (*continued*).

Guanxian–Anxian Fault (F3) and Pingwu–Qingchuan Fault (F4) (see Fig. 1). The earthquake was triggered by a massive crust displacement along the Yingxiu–Beichuan Fault (F2) (Zhang et al., 2008). Two major surface zones ruptured during the earthquake, one developed along the pre-existing Yingxiu–Beichuan Fault (F2) with length of 230 km called Beichuan rupture zone, and the other along the pre-existing Guanxian–Anxian Fault (F3) with length of 70 km called Hanwang–Bailu rupture zone (see Fig. 1). In addition a short rupture zone striking NW called Xiaoyudong rupture zone links the two major rupture zones at the southern end of the Guanxian–Anxian Fault (F3) (Xu et al., 2009).

Historically, earthquakes frequently occurred in the adjacent area of the LMS zone. Eight earthquakes larger than 7.0 Richter Scale have been recorded within the range of 200 km distance from the epicenter of the Wenchuan Earthquake (see Fig. 1). The most intensive earthquake with 7.5 Richter Scale occurred in Diexi County in Sichuan in 1933 (Chen et al., 2008).

The Cenozoic deformation of the LMS, including the active faulting related to the Wenchuan Earthquake, is superimposed on a pre-existing Mesozoic orogen (Burchfiel et al., 1995). Mesozoic deformation in the LMS took place in Late Triassic and Jurassic time, when two distinct structural sequences were deformed and juxtaposed by thrust faulting. The autochthonous lower sequence consists mainly of late Precambrian basement rocks overlain by an incomplete section of latest Proterozoic to Middle Triassic shallow-water sedimentary rocks and Upper Triassic–Jurassic clastic rocks that appear to be foredeep basin deposits and grade eastward into finer-grained strata in the Sichuan Basin. The eastern part of the upper structural sequence has a Precambrian crystalline basement overlain by a thick succession of latest Proterozoic to Lower Triassic shallow-water, highly metamorphosed sedimentary rocks. The western part of the upper sequence consists of up to 10 km of Middle to Upper Triassic flysch, which extends across a broad area of eastern Tibet as the Songpan Garze flysch. This upper structural sequence was imbricated and emplaced eastward over the lower structural sequence in Late Triassic to Middle Jurassic time (see Burchfiel et al., 2008 and Fig. 3).

The Mesozoic thrust complex and its underlying autochthon were refolded and thrust eastward in Cenozoic time. Eocene and probable Oligocene red beds are deformed by northeast-trending folds and thrust faults that merge northward into the LMS along the southwestern margin of the Sichuan Basin. At the north end of the Pengguan massif, the plunging fold that involves basement also folds the overlying Mesozoic thrust complex. The large scale Cenozoic structure of the LMS appears to be similar to that of a fault propagation fold that has been strongly modified by faults (Burchfiel et al., 2008). External structures of the LMS merge with those of the western Sichuan Basin. Folds in the Sichuan Basin are underlain by a décollement that continues to the west beneath the folds of the eastern LMS (Burchfiel et al., 2008).

The tectonics and strata system of the area is very complex as indicated above. In order to understand the strata system of the area, a simplified strata system in the study area was given in Table 1. Fig. 3 indicates that Jurassic and Cretaceous strata are overlain by Quaternary alluvium in the Sichuan Basin to the southwest of the LMS active fault zone, and disclosed in Anxian–Jiangyou of the Sichuan Basin to the northeast of the LMS active fault zone. Triassic strata is wildly outcropped in the western of the study area i.e. Lixian, Maoxian, Beichuan, Pingwu and Wenchuan; meanwhile, along the LMS, there is also a stripe of Triassic strata outcropped, mainly with carbonate rock i.e. limestone and clastic rock i.e. mudstone and sandy mudstone interlayering with silty sandstone and fine sandstone. Permian–Devonian strata is sparsely outcropped in study area, mainly with carbonate rock intercalated clastic rock i.e. slate, carbonate shale. A metamorphic stratum of Silurian is wildly outcropped in Qingchuan County, mainly with marine facies clastic rock, siliceous rock, carbonate rock, flysch and volcanic clastic rock. Ordovician strata and Cambrian strata, with thin-middle thick argillaceous limestone, black siliceous phyllite, black silicalite intercalating siliceous slate, are clustered outcropped in the LMS fault zone with a small area. Sinian strata is mainly outcropped in Qingchuan, and sparsely outcropped in other places i.e. Mianzhu and Maoxian. Archean strata, is mainly outcropped in Anxian, Wenchuan, Mianzhu, Pengzhou and Lixian as shown in Fig. 3. The part outcropped in Wenchuan–Mianzhu, the southwest of the LMS fault, in which the main shock epicenter located, is named as famous “Pengguan massif”, mainly with a set of migmatized metamorphic rock and migmatite.

The study area includes two topographic units, i.e. LMS mountainous area and Chengdu plain. It is located in the transitional region

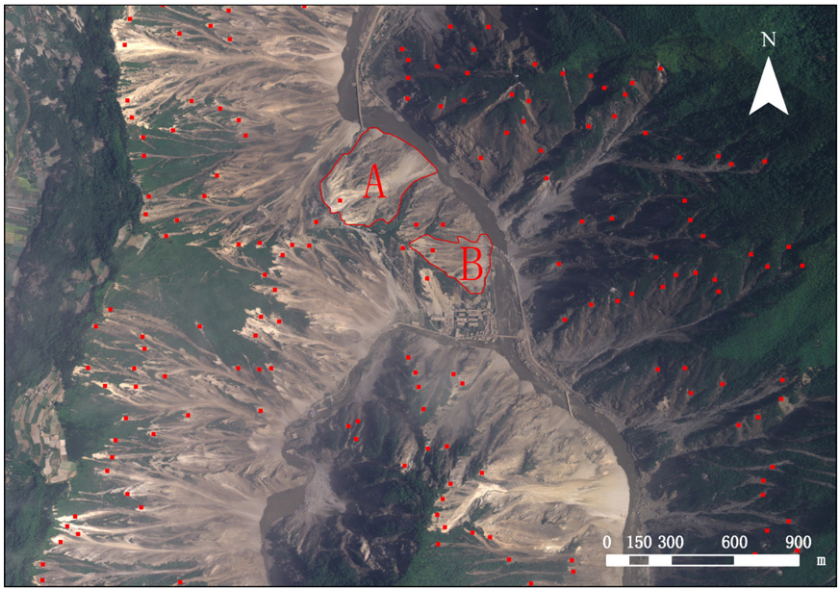

Fig. 5. Example of landslides occurring densely in one site without distinct boundaries and landslide A and landslide B shown on image represent two clusters of landslides.

whose topography varies abruptly from the first steep and rugged topographic step of China, i.e. Qinghai–Tibet Plateau, to the relatively mild second step, i.e. Sichuan basin. LMS Mountainous area, characterized by high mountains and deep valleys, is located in the west and the relative flat Chengdu plain in the east. The southwest part of this area is higher than the northeast part. Mountains in the south of the southwest part are generally 2500–3500 m high above sea level with the highest at 4000 m; mountains in the north of the southwest part are generally 2500–4000 m high with the highest of about 4984 m. The northeast part is about 1500–2500 m high with the highest at 3000 m. The Chengdu plain is overall lower than 800 m in elevation. The local topographic relief in the LMS zone can reach 4000 m within a horizontal distance of less than 50 km making this region one of the steepest slope gradient zone in the world (Fu et al., 2009).

Fig. 4a is a digital elevation model (DEM) of the study area with mesh size of 30 m × 30 m. According to topographical distribution characteristics, the study area is divided into five elevation categories, i.e. <800 m, 800–1200 m, 1200–2000 m, 2000–3000 m, and >3000 m. Statistically, the five categories account for 14.93%, 12.14%, 23.00%, 21.13% and 28.80% of the study area respectively. More than 25% areas with elevation above 3000 m are distributed in the southwest including the Wenchuan County, Lixian County, Maoxian County (see Fig. 4a). The study area is also divided into five categories based

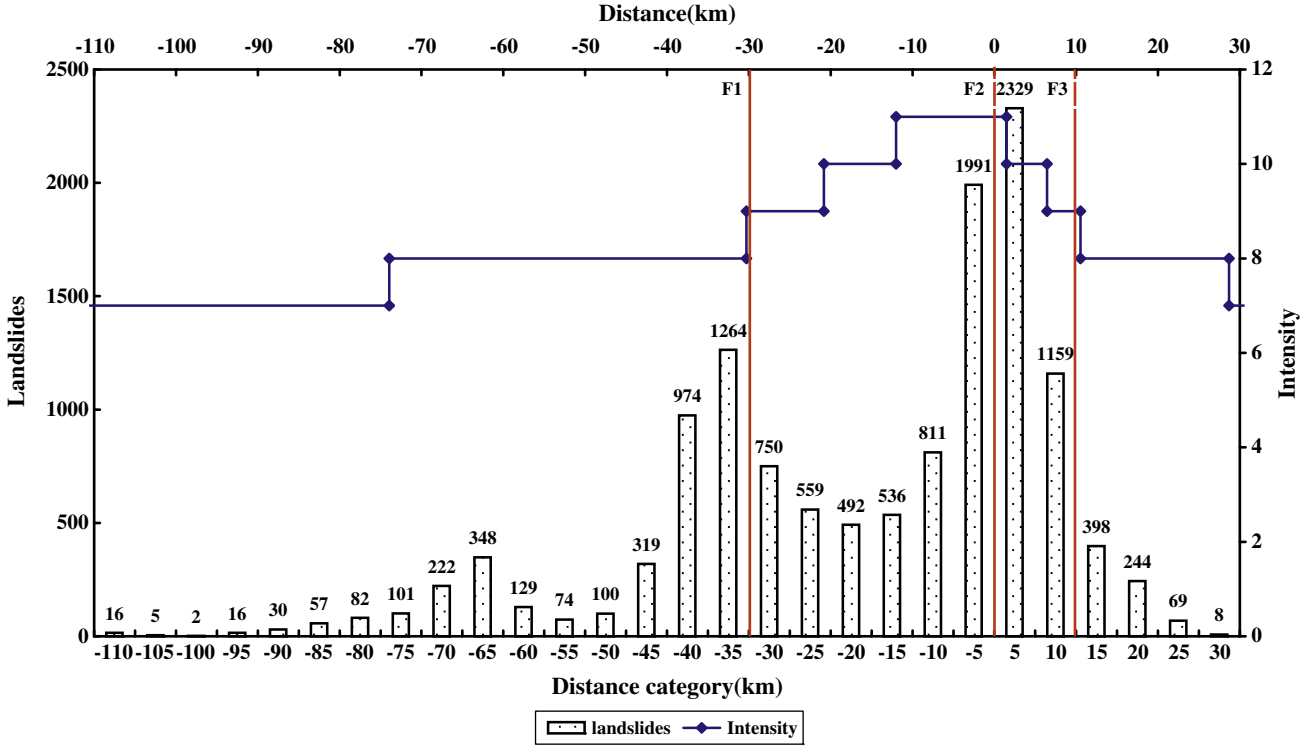

Fig. 6. Variation of landslides cases with distance to the causative fault of F2 and seismic intensity.

on the slope gradient, i.e., 0°–10°, 10°–20°, 20°–30°, 30°–40°, 40°–50°, 50°–60°, 60°–70°, the category of 20°–30° and 30°–40° cover 30.5% and 28.7% of the study area respectively, the category of 50°–60° and 60°–70° cover an area less than 1% of the study area (see Fig. 4b). Slope aspect is almost evenly distributed (see Fig. 4c).

3. Methodologies

"Landslide" is a general term defined as downslope movement of a mass of soil and rock material (Cruden, 1991). Numerous landslide classifications based on morphology, material, mechanism of initiation, or other criteria have been proposed. Based on the principles and terminology of Varnes (1978), Keefer (1984) classified earthquake induced landslides into 14 types. In this paper, we just want to discuss the general distribution features of the earthquake induced landslides and don't want to distinct different types of landslides and discuss the difference.

Concerning different resolution satellite imagery i.e. SPOT and high resolution air photos applied for landslide inventory would damage to its quality, more than 85% of the study area was interpreted with high resolution airphotos, and only a very small part area adopted other satellite images, as shown in Fig. 2. Meanwhile, the smallest landslide in this inventory covers an area of 306.5 m^2 (a little bigger than 16 m × 16 m), and can be easily told from SPOT-5 images. Individual boulders rock falls are not accounted in this study. Therefore the quality of the landslide inventory can be ensured.

A number of landslides clustered occurred in one site without boundaries cannot be discerned and be recorded as one case of landslide. For example, Fig. 5 shows the interpretation result of one part of aerial photo, and dots on the images represent landslides. And point A and point B on the image represent a cluster of landslides respectively. Thus the number of landslides used in the paper should be a little less than the real number of landslides.

Fig. 3 presents the distribution of landslides induced by 2008 Wenchuan Earthquake in the study area. According to the statistical analysis, it is found that there are 13,085 landslides with the total area of about 418.85 km^2.

4. Correlation between landslides induced by the earthquake and geological settings

4.1. Correlation between landslides and active faults

The references indicated that the landslides triggered by earthquake are tending to be distributed in grouping cluster along the causative fault (Keefer, 2000, 2002; Khazai and Sitar, 2003; Huang and Li, 2009), and this is another case. Fig. 3 indicates that the landslides are distributed primarily along the causative faults of Yingxiu–Beichuan Fault (F2) and Guanxian–Anxian Fault (F3). Fig. 6 is the frequency histogram of landslides occurring within every 5 km distance to the surface rupture along the Yingxiu–Beichuan (F2) caused by the earthquake, and the values of the coordinate on the horizontal axis stand for landslides distance to F2, for example the value of 15 stands for landslides distances to F2 in the category of 10–15 km; meanwhile, the locations of the other two faults F1 and F3 are also annotated. It can be seen from Fig. 6 that the number of landslides is decreasing with increasing of distance to the causative fault F2, and 6290 landslides occurred within the buffer zone of −10–10 km distance to faults or surface ruptures, accounting for about 47.3% of the total landslides in the study region. This reflects that the shaking motion is decreasing in general with increasing of distance to the causative fault, which is consistent with conclusions of references, i.e. Keefer (2000, 2002), Khazai and Sitar (2003) et al.

However, more landslides occurred in the block located between F2 and F3 than that in the hanging wall of the causative fault of F2, which is different from the 1999 Chi-Chi Earthquake (Khazai and Sitar, 2003) and the 1989 Loma Prieta event (Keefer, 2000). This is maybe the result of resonance of the block between F2 and F3 under the combination movement of the causative faults F2 and F3 and then the motion there is amplified.

Fig. 6 also indicates that there is an obvious increase in landslide incidence to the adjacent zone of F1, especially the west, which is 30–35 km far away from the fault of F2 and free with surface rupture (see Figs. 6 and 1). This maybe the result that rock mass in the adjacent zone of the active fault is rather fractured, therefore landslide incidence there is a little larger. Meanwhile, the fault F1 is an inverse fault with the hanging wall in the west, the rock mass more fractured in the hanging wall, thus there is an increase in landslide incidence to the west of the active F1.

Statistics also show that there likely exists strong correlation between landslides and the movement of coseismic ruptures within a certain distance. The Beichuan rupture zone shows both uplift offset due to thrusting and slip offset due to horizontal shearing on an en echelon pattern (Xu et al., 2009). Two typical sites are selected: one is the westward of the Beichuan rupture zone in Yingxiu town of

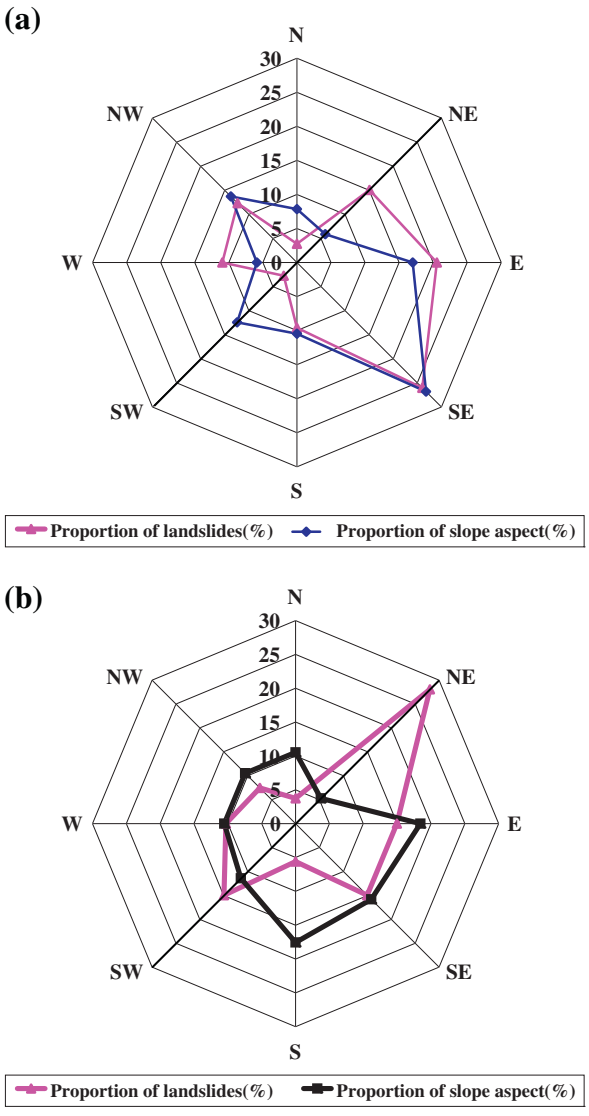

Fig. 7. Distribution of the initial sliding directions and slopes aspects of the landslides in the 10 km concentric band extending outward from Beichuan rupture zones (the solid line from SW–NE represents the striking direction of the ruptures). (a) In epicenter area of Yingxiu town where the rupture zone is dominated by thrust (enveloped by dash line in Fig. 1), (b) In Qingchuan County where the rupture zone is dominated by right lateral slip (enveloped by dash line in Fig. 1).

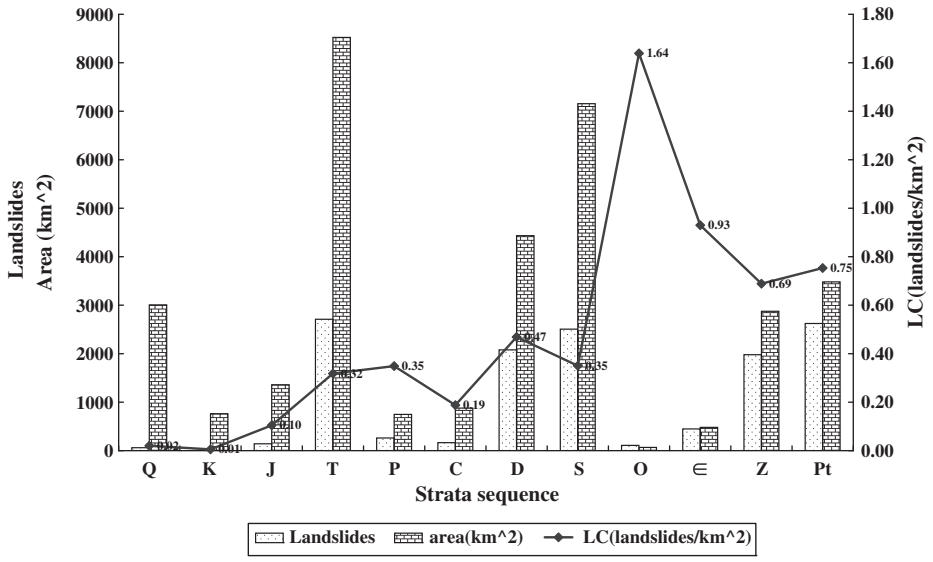

Fig. 8. Relationship between landslides and the strata (rock type see Table 1).

Wenchuan County, where the thrust offset is dominant with mean thrust offset of 3–4 m and the mean right lateral slip offset of 1–2 m; the other is the eastward of the Beichuan rupture zone in Qingchuan County, where the right lateral slip offset is dominant with mean slip offset of 2–4 m and the mean thrust offset of 1–3 m (Xu et al., 2009). Radar pictures of initial sliding directions of the landslides occurred and slopes aspects within the 10 km concentrated band extending outward from Beichuan surface rupture zone (enveloped by the red dash line in Fig. 1) of the two sites are shown in Fig. 7a and b. It can be inferred from Fig. 7 that the dominant initial sliding direction of the landslides is almost same to the movement direction of the causative faults. For example, in the section of Yingxiu town of Wenchuan County most of the landslides have the initial sliding direction of SE, which is the thrust direction of the Beichuan rupture zone in this region; while in the section of Qingchuan County most of landslides have initial sliding direction of NE, which is the striking slip direction of the Beichuan rupture zone. There is no obvious relationship has been found between the initial sliding direction of the landslides and slopes aspects (see Fig. 7a and b). This is maybe the result of the strong inertia force from movement of the causative faults in the near field.

4.2. Correlation between landslides and the lithology

Fig. 8 is the statistics result of correlation between landslides triggered by the 2008 Wenchuan Earthquake and the lithology, which shows that landslides mainly occurred in the strata of Tertiary system (T), Archean (Pt), Silurian system (S), Devonian system (D), and Sinian system (Z), accounting for more than 92% of the total landslides.

To describe the incidence of the landslide in various strata, the index of landslide concentration (LC) — expressed as the number of landslide sources per square kilometer of surface area according to Keefer (2000) is introduced here. It can be indicated from Fig. 8 that the Ordovician system (O) with the least outcropped area has the highest LC of 1.64 landslides/km^2, and Cambrian (∈) system with the second least outcropped area has the second highest LC of 0.93 landslides/km^2. Archean (Pt) strata with lithology of "Pengguan massif" have the third highest LC value of 0.69 landslides/km^2. This is the result of that almost all of the strata of Ordovician system (O), the strata of Cambrian (∈) and main part of Archean (Pt) strata are clustered around the fault rupture zone, rock masses are extremely fractured and the shaking is strong (see Figs. 3 and 9).

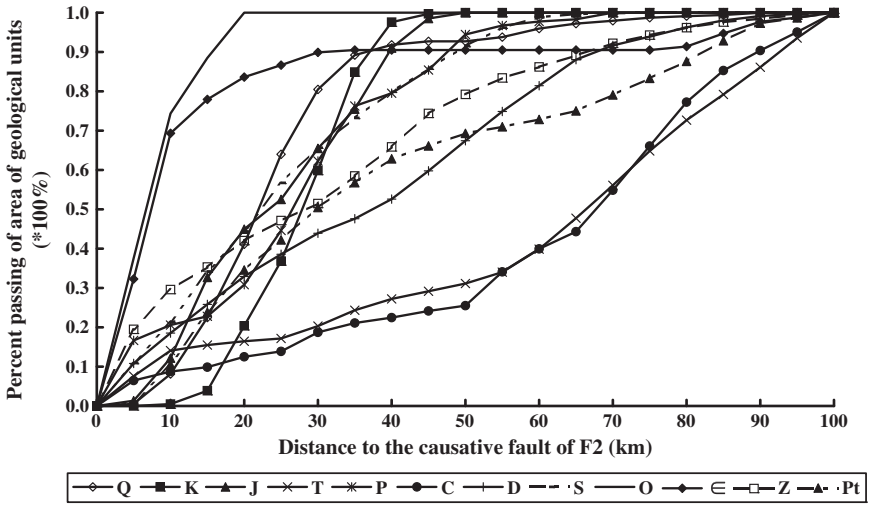

Fig. 9. Percent passing of area of various geological units vs. distance to the causative fault of F2.

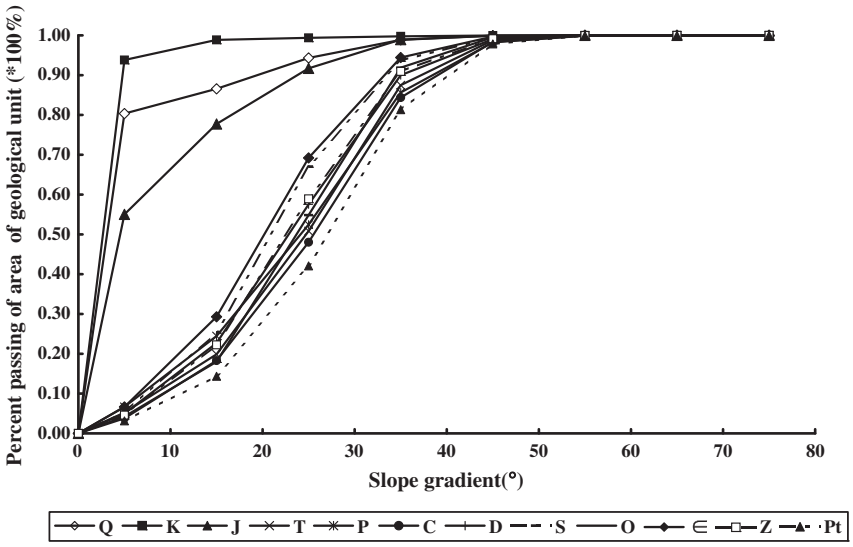

Fig. 10. Percent passing of area of various geological units vs. slope gradient.

Almost all cretaceous (K) system is outcropped in the frontier region of Sichuan Basin (see Fig. 3), with almost flat to gentle slope gradient of 5°–10° (see Fig. 10) and not prone to landslides, as a result, it has the lowest LC value of 0.005 landslides/km^2. Main part of the Quaternary system (Q) has almost flat to gentle slope and not prone to slide in the frontier of Sichuan Basin (see Fig. 3); however, some part of the Quaternary system is distributed in the side slopes of rivers valleys (see Fig. 3) and has more steeper slopes than that of Cretaceous (K) system, which can be also inferred from that the curve of percent passing of area of Cretaceous (K) system has a more steeper slope from 5°–10° (see Fig. 10). As a result the Quaternary system has the second lowest LC value of 0.02 landslides/km^2.

4.3. Correlation between landslides and the topography

The relationship between landslides and the corresponding slope gradient categories has been examined as shown in Fig. 11. Landslides increase with increasing the slope gradient until the maximum is reached in the 30°–40° category, and then decreases generally with increasing the slope gradient; however the LC shows an increase trend with slope gradient increasing and reaches its biggest in the category of 50°–60°, and then decrease a little in the category of 60°–70° (see Fig. 11). The absence of landslides in steeper slope categories is mainly due to the small number of such cells, which together cover less than 0.04% of the total surface area.

Once the median value of each slope gradient category is adopted, the data of LC and tangent of slope angle are fit well by an exponent regression line $LC = 0.2234e^{0.7234\tan\theta}$ with $R^2 = 0.5608$ (see Fig. 11), where LC is landslides in per square kilometer, and θ is slope angle.

According to statistical results, landslides increase with increasing the slope elevation until the maximum is reached in the 1200–2000 m and then decrease; LC has the similar trend and reaches its largest in the elevation category of 800–1200 m (see Fig. 12). The region in the elevation category of <800 m elevation mainly distributed in the margin area of Sichuan Basin with flat to gentle slope gradient and then not prone to slide (see Figs. 4a and 13). The region in the elevation of 800–2000 m has five terraces and experienced fast river incision with thin valleys (Kirby et al., 2000; Zhang et al., 2005), and the slopes have steeper gradient and prone to fail, and then landslides and LC has its largest in this category. The region above 2000 m elevation mainly dominates with wide valleys (Kirby et al., 2000; Zhang et al., 2005). Meanwhile, Fig. 14 indicates that the category of

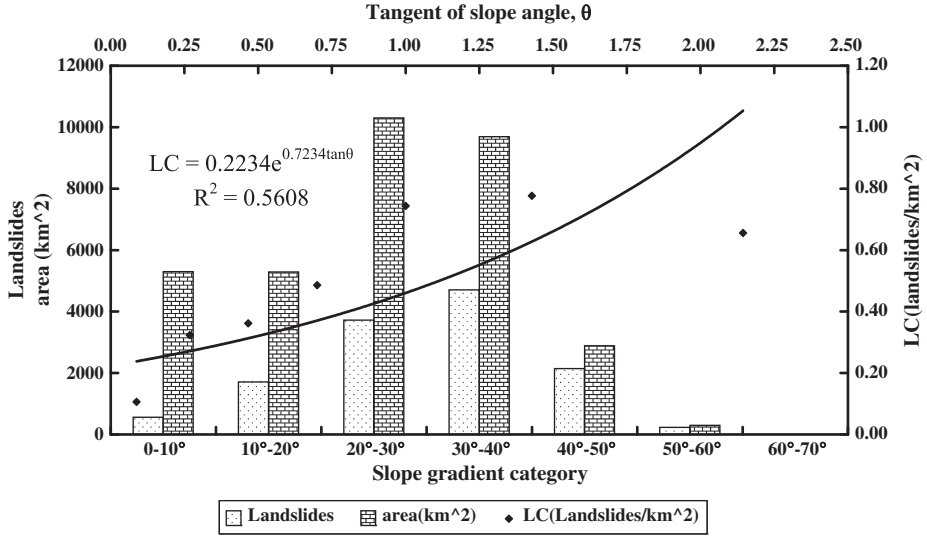

Fig. 11. Histogram of landslides in various slope gradient categories.

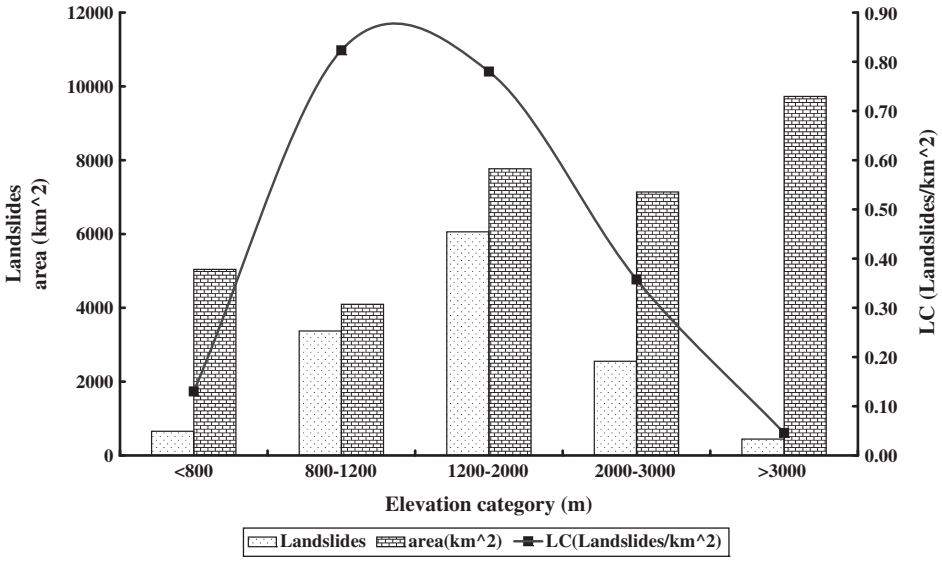

Fig. 12. Histogram of landslides in various elevation categories.

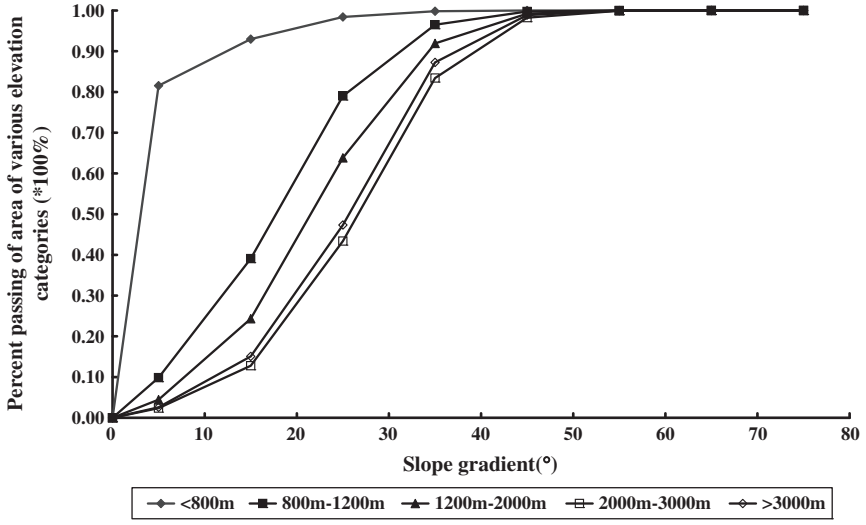

Fig. 13. Percent passing of area of various elevation categories vs. slope gradient.

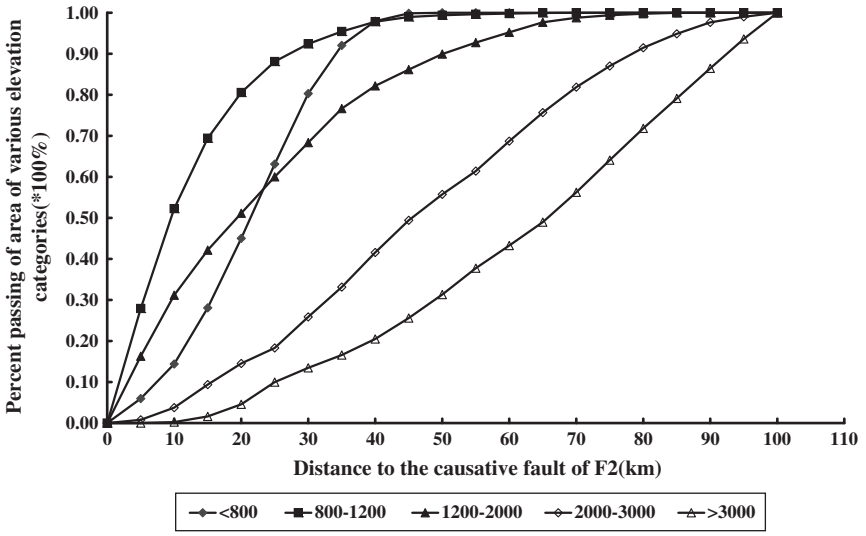

Fig. 14. Percent passing of area of various elevation categories vs. distance to the causative fault of F2.

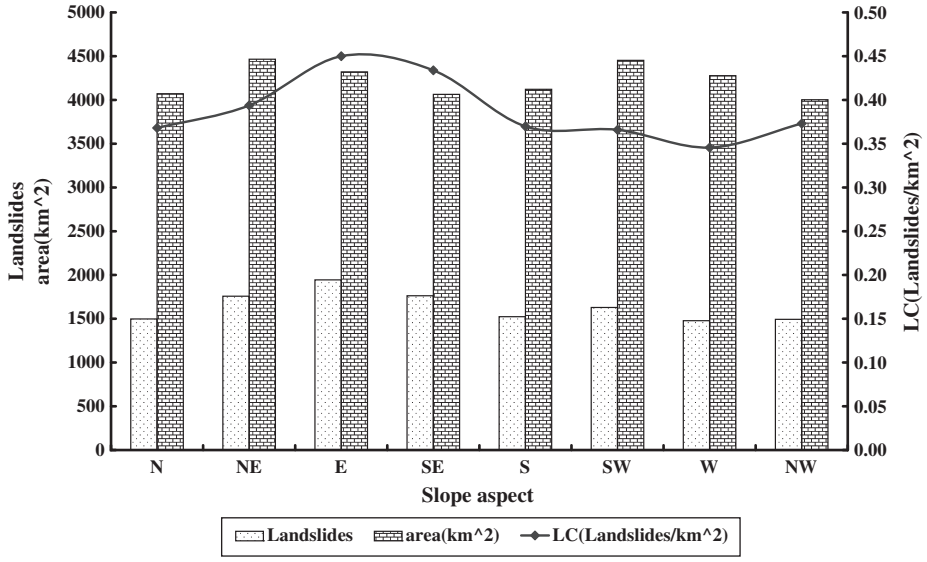

Fig. 15. Histogram of landslides in various slope aspects.

2000–3000 m and >3000 m elevations are mainly distributed in the west margin of the study area, with a larger distance to the causative faults. These are maybe the main reasons lead to the distribution form of the landslides with various elevation categories.

Statistics also indicates that landslides triggered by 2008 Wenchuan Earthquake is evenly distributed in eight slope aspects, and LC has a slightly higher value in E and SE direction than any others (see Fig. 15), which maybe indicates that slope aspect has minor influence on the distribution of the landslides triggered by earthquake.

5. Discussions

The statistics analysis above indicates that the distribution of the Earthquake triggered landslides generally decreases with the increasing distance to the causative fault, and an obvious increase in landslide incidence occurred locally in the adjacent active faults zone in which rock masses are always extremely fractured. There is no obvious correlation has been found between LC and the geological unit, and LC values in different geological unit may have been affected by slope gradient for each unit and distance of each unit to causative fault zone (see Figs. 10 and 9). LC has a good exponent regression expression with tangent of slope gradient. LC values in different elevation category may have been also depended on slope gradient for each elevation category (which has close relationship with the topography evolution of the region) and distance of each category to causative fault zone (see Figs. 13 and 14). Slope aspects may have little influence on the distribution of the landslides and LC as well. The distance to causative fault and slope angle have more important influence on the distribution of the landslides triggered by earthquake and LC than any other geological setting factors motioned above.

The intensity of an earthquake reflects that the observations of damaged structures and the presence of secondary effects, such as earthquake induced landslides, liquefaction, and ground cracking. Isoseismal map from CEA (2008) is plotted in Fig. 1. Statistics indicates that all landslides occurred in the area with seismic intensity above VI (see Fig. 16); meanwhile, the curve of LC shows an obvious increase above VIII, and LC reaches its summit of 1.31 landslides/km^2 in XI region from a value of 0.21 landslides/km^2 in VIII region (see Fig. 16). Therefore in mountainous area, LC can be acted as an important index to draw isoseismal map, not the number of landslides.

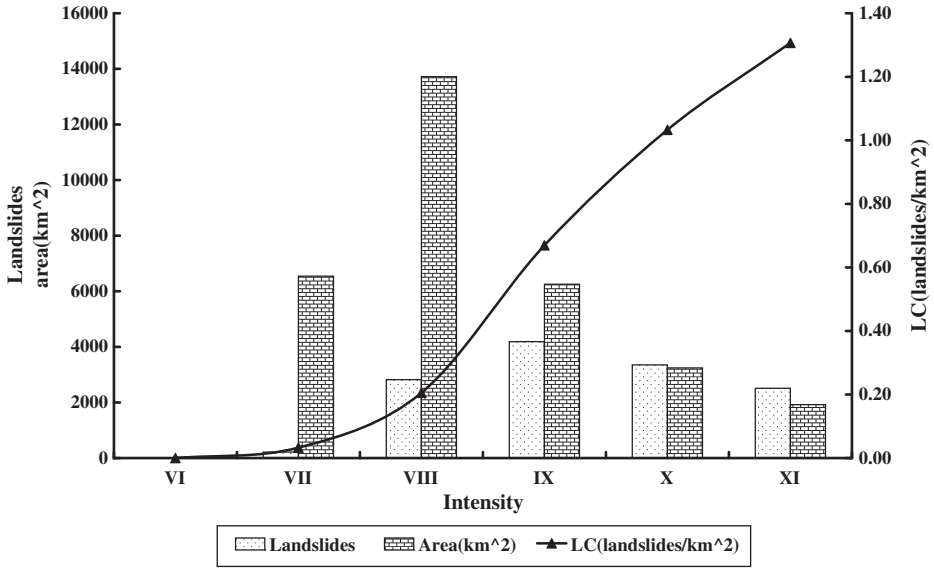

Fig. 16. Relationship between landslides and the seismic intensity.

It has been found during field investigations that landslide incidence has close relationship with the structure of the slope. Landslides events in layered slopes closely depend on the angle β between dipping direction of the slope and the dipping direction of the bedding planes. Preliminary study indicates that the larger the angle β is, the lower the frequency of landsliding incidence is. The lowest landsliding incidence exists in slopes whose dipping directions are normal to the dipping direction of the bedding plane. Taking a site of Beichuan as shown in Fig. 17 for example, the right slope has the angle β of about 80–90° (Fig. 17a), and the left slope is a consequent slope (Fig. 17b). It can be seen from Fig. 17 that the while the right slope kept stable, the left slope failed (named as Magongyan landslide) during the earthquake and blocked up the river. Similar phenomena can also be found in the study area. Consequent slopes and obsequent slopes are more prone to slide, for example, the well known Tangjiashan landslide, Daguangbao landslide, Laoyingyan landslide and Magongyan landslide occurred in the consequent slope, and Xiaojianping landslide and Chenjiaba landslide took place in obsequent slopes.

Slope structure also has influence on form of the failure. For example, blocky slopes tend to fail in the form of rock fall, rock avalanche and rock slide due to the development of discontinuities, i.e. Noujuangou landslide (see Fig. 18); eluvium and colluvial layer of slopes tend to have many shallow landslides and rock falls (see Fig. 19); and slopes with fragile structures tend to have numerous rock block falls.

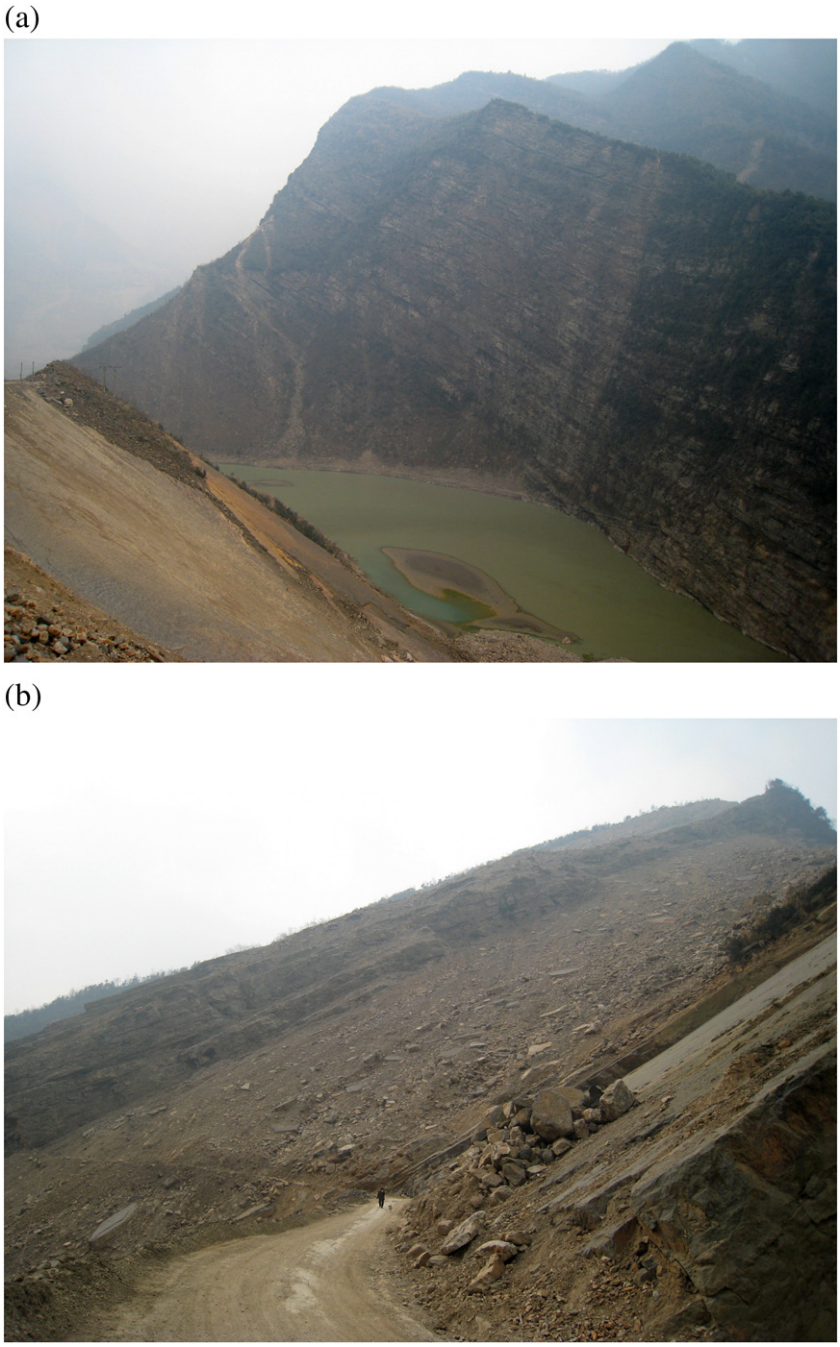

Fig. 17. (a) The right slope with striking direction almost normal to striking direction of the bedding plane kept stable while the left consequent slope failed during the earthquake (With camera pointing to N); (b) The left consequent slope failed — Magongyan landslide (With camera direction of 195°).

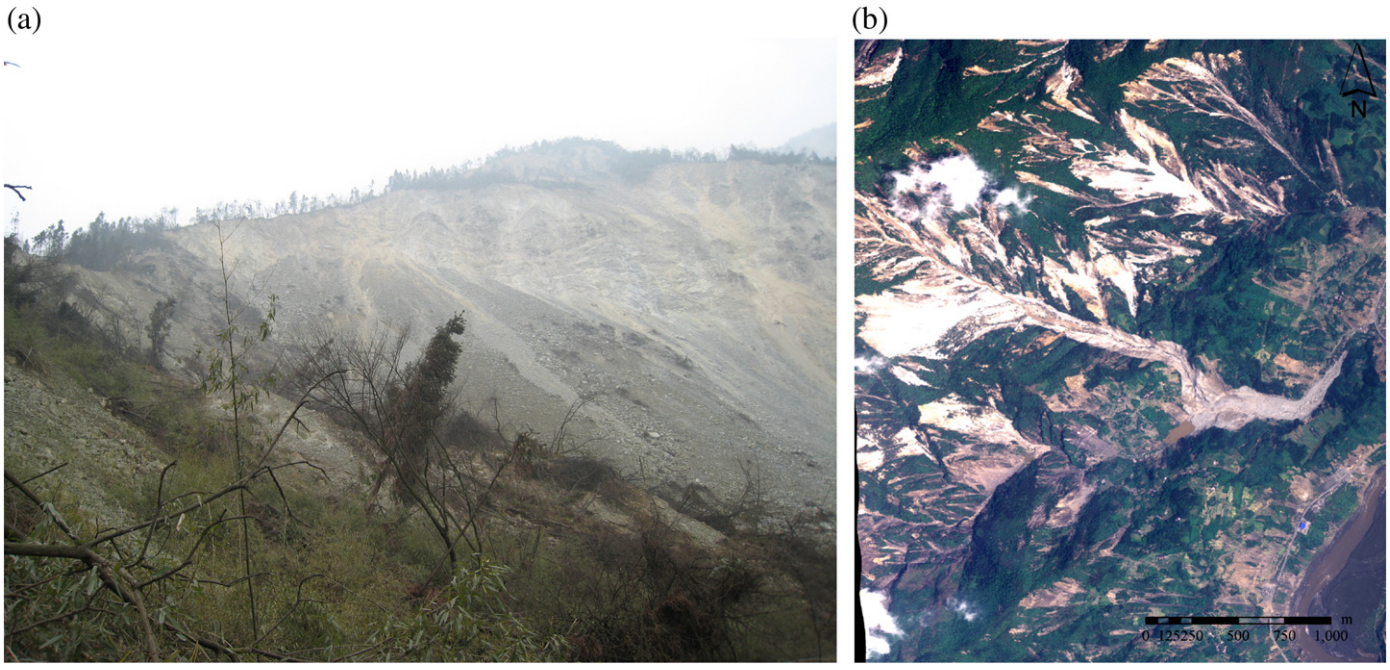

Fig. 18. (a) The source characteristics of Niujuangou landslide with camera direction of 300°, occurred in blocky slopes (Qi et al., 2010); (b) the aerial photo of Niujuangou landslide (Qi et al., 2010).

Fig. 19. Shallow landslides occurred in eluvium and colluvial layer of slopes (with camera direction of 290°).

6. Conclusions

With landslides database built by means of the interpretation of RS data and field investigations, the correlations between the landslides and geological settings i.e. active faults (the coseismic surface ruptures), geological unit, and topography are detailed, and distribution features of the landslides induced by 2008 Wenchuan Earthquake are presented as follows:

(1) The landslides are dominantly developed along the LMS fault zone. About 47.3% of landslides in the study region occur within the buffer zone of −10–10 km distance to faults or surface ruptures. The landslides are not only clustered around the causative faults with surface ruptures i.e. F2 and F3, but also the active faults adjacent to the causative faults i.e. F1. Moreover, it has been noticed that most of the landslides have the initial sliding directions almost same to movement direction of the causative faults within the 10 km concentrated band extending outward, which is maybe the result of the strong inertia force from movement of the causative faults in the near field.

(2) LC differs substantially among various geologic units in the study area. LC has its lowest and its second lowest in the area

outcropped with strata of Cretaceous (K) system and Quaternary (Q) system, and has its largest and second largest in the strata of Ordovician system (O) and Archean (Pt) respectively. LC doesn't show obvious correlation with the geological unit. The difference of LC value in geological unit may have been affected by slope gradient for each unit and distance of each unit to causative fault zone.

(3) LC shows an exponent increase with slope gradient, which is consistent with the conclusion presented by Keefer (2000). LC doesn't have obvious relationship with the elevation category, and the difference of LC in each elevation category may have been closely related with the distance of each unit to causative fault zone and the topography evolution in the region (slope gradient for each unit). Slope aspects may have little influence on the distribution of the landslides and LC as well.

(4) The distributed landslides triggered by earthquake are mainly depended on the distance to the causative faults and slope gradient.

(5) Isoseismal map reflects the incidence of landslides in some degree, and LC increases dramatically with Intensity increasing, almost all landslides occurred in the region above VI degree.

Acknowledgements

Immediately after Wenchuan Earthquake, the authors from Chinese Academy of Sciences (CAS) took part in the project team of Remote Sensing Monitoring and Assessment of Wenchuan Earthquake which was initiated by experts from seven institutes of CAS, and took charge of the interpretation of geological hazards. This paper is completed based on this work. Meanwhile, the authors wish to thank the financial supports from Chinese Academy of Sciences under grants of KKCX1-YW-01 and KKCX1-YW-04, State Key Laboratory of Geo-hazard Prevention & Geo-environment Protection under grant of DZKJ-0802, and One Hundred Talents Program of Chinese Academy of Sciences. The authors thank the kind assistance from Master's degree candidates Feng Cao, Song Lin, Zengbo Zhou, and Ph.D candidates Shangmin Zhao and Rulin Ouyang who come from Institute of Geographic Sciences and Natural Resources Research, CAS for processing the DEM, Miss Xiaowei Shi and Chunling Liu for processing of the data, Dr. Jianfeng Chai for kindly checking the language of the paper. The authors also would like to give great thanks to Professor Bill Murphy and another anonymous reviewer for thoughtful and constructive comments, which greatly improved the quality of the manuscript.

References

Burchfiel, B.C., Chen, Z., Liu, Y., Royden, L.H., 1995. Tectonics of the Longmen Shan and adjacent regions. International Geology Review 37, 661–738.

Burchfiel, B.C., Royden, L.H., van der Hilst, R.D., Chen, Z., King, R.W., Li, C., Lü, J., Yao, H., Kirby, E., 2008. A geological and geophysical context for the Wenchuan earthquake of 12 May 2008, Sichuan, People's Republic of China. GSA Today 18. doi:L10.1130/GSATG18A.1.

Chen, Xiaoqing, Cui, Peng, Cheng, Zunlan, You, Yong, Zhang, Xiaogang, He, SiMing, Dang, Chao, 2008. Emergency risk assessment of dammed lakes caused by the Wenchuan earthquake on May 12, 2008. Earth Science Frontiers 15 (4), 244–249 (In Chinese with English abstract).

China earthquake administration — CEA, 2008. Ioseismal map of the Wenchuan earthquake. http://www.cea.gov.cn/manage/html/8a8587881632fa5c0116674a018300cf/_content/08_08/29/1219980517676.html2008.

China Geological Survey, CGS, 2001. Regional geological map of Sichuan Province (1:200, 000), Geological Press.

Copley, A., McKenzie, D., 2007. Model of crustal flow in the India–Asia collision zone. Geophysical Journal International 169, 683–698. doi:L10.1111/j.1365-246X.2007.03343.x.

Cruden, D.M., 1991. A simple definition of a landslide. Bulletin of the International Association of Engineering Geology 43, 27–29.

Fu, B.H., et al., 2009. Atlas of Seismological and Geological Disasters Associated with the 12 May 2008 Ms 8.0 Wenchuan Great Earthquake, Sichuan, China. Seismological press, Beijing. (In Chinese and In English).

Geological Bureau of Sichuan Province, 1991. Geological Topology of Sichuan Province. Geological Press, China.

Houseman, G., England, P., 1993. Crustal thickening versus lateral expulsion in the Indian–Asian continental collision. Journal of Geophysical Research 98, 12,233–12,249. doi:L10.1029/93JB00443.

Huang, R., Li, W., 2009. Analysis of the geo-hazards triggered by the 12 May 2008 Wenchuan Earthquake, China. Bulletin of Engineering Geology and the Environment 68, 363–371.

Jiang, X., Yu, J., 2005. Mapping the deep lithospheric structure beneath the eastern margin of the Tibetan Plateau from gravity anomalies. Journal of Geophysical Research 110, B07407. doi:L10.1029/2004JB003394.

Keefer, D.K., 1984. Landslides caused by earthquakes. Geological Society of America Bulletin 95, 406–421.

Keefer, D.K., 2000. Statistical analysis of an earthquake-induced landslide distribution — the 1989 Loma Prieta, California Event. Engineering Geology 58, 213–249.

Keefer, D.K., 2002. Investigating landslides caused by earthquakes—a historical review. Surveys in Geophysics 23, 473–510.

Khazai, Bijan, Sitar, Nicholas, 2003. Evaluation of factors controlling earthquake-induced landslides caused by Chi-Chi earthquake and comparison with the Northridge and Loma Prieta events. Engineering Geology 71, 79–95.

Kind, R., Yuan, X., Saul, J., Nelson, D., Sobolev, S.V., Mechie, J., Zhao, W., Kosarev, G., Ni, J., Achauer, U., Jiang, M., 2002. Seismic images of crust and upper mantle beneath Tibet: evidence for Eurasian plate subduction. Science 298, 1219–1221. doi:L10.1126/science.1078115.

Kirby, E., Whipple, K.X., Burchfiel, B.C., et al., 2000. Neotectonics of the Min Shan, China: implications for mechanisms driving Quaternary deformation along the eastern margin of the Tibetan Plateau. GSA Bulletin 112 (3), 375–393.

Li, C., van der Hilst, R., Meltzer, A.S., Engdahl, E.R., 2008. Subduction of the Indian lithosphere beneath the Tibetan Plateau and Burma. Earth and Planetary Science Letters 274, 157–168. doi:L10.1016/j.epsl.2008.07.016.

Molnar, P., Chen, W., 1978. Evidence for large Cenozoic crustal shortening of Asia. Nature 273, 218–220. doi:L10.1038/273218a0.

Molnar, P., Tapponnier, P., 1975. Tectonics in Asia: consequences and implications of a continental collision. Science 189, 419–426. doi:L10.1126/science.189.4201.419.

Qi, S., Xu, Q., Liu, C., Zhang, B., Liang, N., Tong, L., 2009. Slope instabilities in the severest in the severest disaster areas of 5.12 Wenchuan Earthquake. Chinese Journal of Engineering Geology 17 (1), 39–49.

Qi, S., Xu, Q., Zhang, B., Zhou, Y., Lan, H., Li, L., 2010. Source characteristics of long runout rock avalanches triggered by the 2008 Wenchuan earthquake, China. Journal of Asian Earth Sciences. doi:L10.1016/j.jseaes.2010.05.010.

Royden, L.H., Burchfiel, B.C., van der Hilst, R.D., 2008. The geological evolution of the Tibetan plateau. Science 321, 1054–1058. doi:L10.1126/science.1155371.

Sato, H.P., Harp, E.L., 2009. Interpretation of earthquake-induced landslides triggered by the 12 May 2008, M7.9 Wenchuan earthquake in the Beichuan area, Sichuan Province, China using satellite imagery and Google Earth. Landslides 6, 153–159. doi:L10.1007/s10346-009-0147-6.

Varnes, D.J., 1978. Slope movement types and processes. In: Schuster, R.L., Krizek, R.J. (Eds.), Landslide Analysis and Control. National Research Council. Transportation Research Board, Washington, DC, pp. 11–13.

Wang, F., Cheng, Q., Highland, L., Miyajima, M., Wang, H., Yan, C., 2009. Preliminary investigation of some large landslides triggered by the 2008 Wenchuan earthquake, Sichuan Province, China. Landslide 6, 47–54.

Xu, L., Rondenay, S., Van der Hilst, R.D., 2007. Structure of the crust beneath the southeastern Tibetan Plateau from teleseismic receiver functions. Physics of the Earth and Planetary Interiors 165, 176–193.

Xu, X., Wen, X., Yu, G., Chen, G., Klinger, Y., Hubbard, J., Shaw, J., 2009. Coseismic reverse- and oblique-slip surface faulting generated by the 2008 Mw 7.9 Wenchuan earthquake, China. Geology 37 (6), 515–518. doi:L10.1130/G25462A.

Yao, H., Beghein, C., van der Hilst, R.D., 2008. Surface-wave array tomography in SE Tibet from ambient seismic noise and two-station analysis: II—Crustal and upper mantle structure. Geophysical Journal International 173, 205–219. doi:L10.1111/j.1365-246X.2007.03696.x.

Yin, Y., Wang, F., Sun, P., 2009. Landslide hazards triggered by the 2008 Wenchuan earthquake, Sichuan, China. Landslides 6, 139–151.

Zhang, P.Z., Shen, Z., Wang, M., Gan, W., 2004. Continuous deformation of the Tibetan Plateau from Global Positioning System data. Geology 32, 809–812. doi:L10.1130/G20554.1.

Zhang, Y., Yang, N., Meng, H., 2005. Deep incised valley along Minjiang River upstream and their responses to the uplift of the west Sichuan plateau. China. Journal of Chengdu University of Technology 32 (4), 331–339.

Zhang, P., Xu, X., Wen, X., Ran, Y., 2008. Slip rates and recurrence intervals of the Longmenshan active fault zone, and tectonic implications for the mechanism of the May 12 Wenchuan earthquake, 2008, Sichan, China. Chinese Journal of Geophysics 51 (4), 1066–1073.